*Korean J. Chem. Eng.*, 17(5), 510-515 (2000)

# Measurement of Bubble Point Pressures and Critical Points of Carbon Dioxide and Chlorodifluoromethane Mixtures Using the Variable-Volume View Cell Apparatus

**Jae Min Lee, Byung-Chul Lee† and Chan-Hwi Cho***

Department of Chemical Engineering, Hannam University, 133 Ojung-dong, Taeduk-gu, Taejon 306-791, Korea
*Department of Chemical Engineering, Youngdong University, Youngdong-kun, Chungbuk 370-800, Korea
(*Received 5 November 1999 • accepted 18 June 2000*)

**Abstract**−The bubble point pressures and the critical points of carbon dioxide ($CO_2$) and chlorodifluoromethane (HCFC-22) mixtures were measured by using a high-pressure experimental apparatus equipped with a variable-volume view cell, at various $CO_2$ compositions in the range of temperatures above the critical temperature of $CO_2$ and below the critical temperature of HCFC-22. The experimental bubble point pressure data were correlated with the Peng-Robinson equation of state (PR-EOS) to estimate the corresponding dew point compositions at equilibrium with the bubble point compositions. The experimentally measured bubble point pressures and the mixture critical points gave good agreement with those calculated by the PR-EOS. The variable-volume view cell equipment was verified to be an easy and quick way to measure the bubble point pressures and the mixture critical points of high-pressure compressible fluid mixtures.

Key words: Bubble Point Pressure, Mixture Critical Points, Carbon Dioxide ($CO_2$), Chlorodifluoromethane (HCFC-22), Variable-Volume View Cell, Peng-Robinson Equation of State

## INTRODUCTION

To experimentally measure the vapor-liquid equilibrium (VLE) data of high-pressure compressible fluid mixtures, it is common to use a circulation-type apparatus equipped with a constant-volume cell [Lim et al., 1997; Nishiumi et al., 1997; Park and Lee, 1997]. However, this conventional equipment has a disadvantage in that it requires a time sufficient to ensure equilibrium during the circulation of the vapor and liquid mixtures. It also requires obtaining samples from the liquid and vapor phases simultaneously and accurately and then analysing their compositions.

On the other hand, a variable-volume view cell apparatus is well-known as a simple and quick way capable of measuring the phase equilibrium behavior of high-pressure compressible fluid mixtures [Haschets and Shine, 1993; Lee et al., 1996; Choi and Yeo, 1998]. The phase equilibrium can be easily measured by changing the volume of the view cell containing the fluid mixture of a known composition and by observing the phase change through the window of the cell. This equipment was originally designed to measure the cloud points of a mixture indicating the phase boundary between single- and two-phases. The advantage of using the variable-volume cell is that the concentration of the system is kept constant during the experiment. On the other hand, using the constant-volume cell often requires venting off solution to decrease the pressure of the system causing unknown changes in the concentration of the cell contents [Irani and Cozewith, 1986].

The main objective of this work was to measure the bubble point pressures and critical points of a high-pressure binary mixture by using the variable-volume view cell apparatus. We chose a carbon dioxide ($CO_2$)/chlorodifluoromethane (HCFC-22) system as the high-pressure compressible fluid mixture and measured its bubble point pressures and critical points at various mixture compositions and in the range of temperatures above the critical temperature of $CO_2$ and below the critical temperature of HCFC-22. It would be valuable to generate the bubble points at temperatures above the critical temperature of $CO_2$ since the only phase equilibrium data available from the literature for the $CO_2$/HCFC-22 system are the VLE data at temperatures below or near the critical temperature of $CO_2$ [Knapp et al., 1982]. It would also be interesting to obtain the equilibrium behavior between the nonpolar $CO_2$ and the polar HCFC-22.

The experimentally measured bubble point data were correlated with the popular Peng-Robinson equation of state (PR-EOS) containing an adjustable binary interaction parameter [Prausnitz et al., 1986]. The vapor phase compositions, i.e., the dew point compositions corresponding to the bubble points, were calculated with the optimum values of the PR-EOS binary interaction parameter. The mixture critical points measured experimentally were compared with those calculated by the PR-EOS.

## EXPERIMENTAL

### 1. Materials

The liquefied gases of $CO_2$ and HCFC-22 were purchased from Myung Sin General Gas Co. (Korea) and Solvey Gas Co. (USA), respectively, and their certified purities were 99.99 wt%. Both of the gases were used without further purification.

### 2. Apparatus

Fig. 1 shows a schematic diagram of the experimental high-pressure apparatus for measuring the bubble point pressures and the mixture critical points for $CO_2$/HCFC-22 system. The experimental apparatus used in this work is similar to that used by Haschets and Shine [1993] and Lee et al. [1996]. The heart of the

†To whom correspondence should be addressed.
E-mail: bclee@mail.hannam.ac.kr

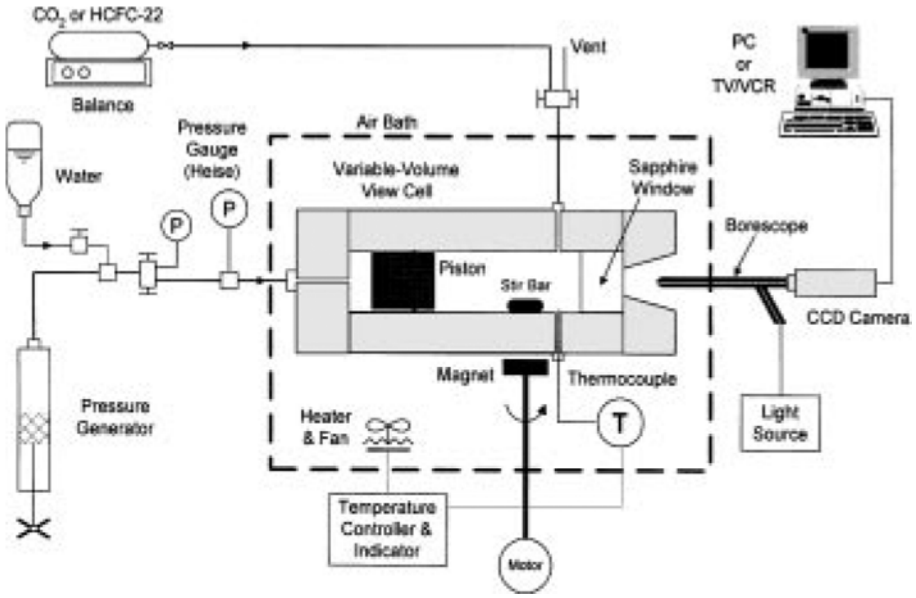


**Fig. 1. A schematic diagram of the experimental variable-volume view cell apparatus for measuring the bubble point pressure and the critical point of a mixture.**

system is the high-pressure variable-volume view cell. The cell has a dimension of 16 mm I.D.×70 mm O.D., and an internal working volume of about 31 $cm^3$. A movable piston is placed inside the cell to change the cell volume. A pressure generator (High Pressure Equipment Co. model 50-6-15, 15,000 psi rating, 20 cc capacity) is used to pressurize water and therefrom displace the piston. A change in the cell volume causes a change of the system pressure. A sapphire window (3/4" diameter×3/4" thick) is inserted into the view cell for visual observation of the interior of the cell. O-rings and back-up rings create seals between the end caps and the cell body, and between the piston and the inner wall of the cell.

The system pressure is measured with a high-precision pressure gauge (Dresser Heise model CC-12-G-A-02B, 500 bar max. pressure, ±0.5 bar accuracy) placed between the pressure generator and the view cell instead of being connected directly to the cell. The pressure is measured on the pressurizing fluid (water) side of the piston to minimize the dead volume in the line connecting the cell to the pressure gauge, which can cause an uncertainty in the exact concentration in the cell. The pressure drop was observed to be about 1.3 bar across the piston, and thus in each experiment the bubble point pressure was added by 1.3 bar to account for the pressure drop. The system temperature is measured by an RTD (Pt-100Ω) inserted into the interior of the cell and is read with a high-precision digital thermometer (ASL model F250, ±0.01 °C accuracy). A temperature-controlled forced-convection air bath (Jeio-Tech model FO-600M, 250 °C max. temperature) is used to keep the system temperature constant.

A visual observation of the interior of the cell through the sapphire window is made by a borescope (Olympus model R080-044-000-50) and a CCD camera (WAT-202B) connected to a VCR/TV monitor and a computer. A cold light source (Olympus model ILK-5) is used to provide illumination inside the view cell. A magnetic stirring system is equipped under the cell body to mix the contents in the cell. A stirring bar in the cell is activated by a samarium-cobalt magnet located below the cell, and the magnet is driven by an electric motor and an RPM controller.

**3. Methods**

The experiment for measuring the bubble point pressures and the critical points of the $CO_2$/HCFC-22 mixtures was performed by the following procedure. After assembling a piston, o-rings and a sapphire window into the view cell, we placed the cell inside the air bath to keep the system temperature constant. To remove any entrapped air present in the cell, the cell was purged with a small amount of HCFC-22 gas at least three times. A certain amount of the liquefied HCFC-22 and $CO_2$ was charged into the cell through the inlet line. HCFC-22 was first charged because its vapor pressure was lower than that of $CO_2$. The composition of each component in the mixture was determined by weighing each of HCFC-22 and $CO_2$ sample cylinders with an accuracy of ±0.001 g before and after charging them into the cell.

After water was filled from the pressure generator to the left side of the piston, the solution in the cell was then continuously pressurized by using the pressure generator. As the pressure generator pressurizes water, the compressed water moves the piston to the window side to decrease the cell volume and thus raise the pressure inside the cell. As the pressure increases, the solution in the cell finally becomes a single homogeneous phase. At the same time the solution was well agitated by a stirring bar.

Once the system reached thermal equilibrium and the solution was maintained at a homogeneous single phase, the pressure was then reduced very slowly until tiny vapor bubbles started to form from the single phase solution; the inside of the cell was visually observed through the window. The pressure was decreased by moving the piston back to the water side by using the pressure generator. At a fixed composition and temperature, the bubble point pressure was defined as the initial pressure at which the first bubble was observed. For reproducing consistent measurements, every measurement was repeated at least twice at each temperature. The bubble point pressures at different temperatures and compositions were measured in the same way, changing the temperature of the solution to its critical point. When the solution reaches the critical point, it becomes a little reddish and no bubbles occur even though the pressure decreases. The temperature and pressure at which this phenomenon is observed corresponds to the critical point of the mixture at a given composition. The bubble point pressures and the mixture critical points at different $CO_2$ compositions were measured by the same procedure.

## RESULTS AND DISCUSSION

Table 1 shows the experimental data of the bubble point pressures and the mixture critical points at various $CO_2$ compositions and temperatures for the $CO_2$/HCFC-22 system. The last point of temperature and pressure at each $CO_2$ composition represents the mixture critical point. Fig. 2 shows a P-T diagram of the experimental data of Table 1. The saturated vapor pressure curves of pure $CO_2$ and HCFC-22 were obtained from the Disign Institite for Physical Property Data (DIPPR) data compilation [Daubert and Danner, extent 1994]. The bubble point pressure at a fixed temperature and $CO_2$ mole fraction was defined as the initial pressure at which the first bubble started to form. As the system temperature increased, the bubble point pressure increased and finally ended up at the critical point of the mixture. The line connecting through the critical points at various $CO_2$ compositions indicates the critical locus of the mixtures, which are placed between the critical points of pure $CO_2$ and HCFC-22. Increasing the $CO_2$ composition in the mixture caused an increase in the bubble point pressure of the mixture, since the vapor pressure of $CO_2$ was higher than that of HCFC-22. The slope of the bubble point pressure with respect to temperature, $(\partial P/\partial T)_x$, increased as the $CO_2$ content in the mixture increased.

The bubble point pressures at various temperatures were generated as a function of the $CO_2$ composition by making a polynomial interpolation of Fig. 2. Table 2 shows the results estimated by the interpolation of the bubble point pressures as a function of $CO_2$ mole fraction at several temperatures. As described above, the

**Table 1. Experimental bubble point data for $CO_2$(1)/HCFC-22(2) system**

| Bubble point mole fraction of $CO_2$, $x_1$ | Temperature [°C] | Bubble point pressure [bar] | Bubble point mole fraction of $CO_2$, $x_1$ | Temperature [°C] | Bubble point pressure [bar] |
|---|---|---|---|---|---|
| 0.1036 | 29.0 | 15.1 | 0.5866 | 28.6 | 39.7 |
| | 40.4 | 19.5 | | 35.3 | 44.5 |
| | 50.3 | 24.3 | | 40.7 | 48.8 |
| | 59.5 | 29.5 | | 47.7 | 54.8 |
| | 59.9 | 29.8 | | 52.5 | 59.8 |
| | 70.0 | 36.7 | | 57.8 | 65.0 |
| | 79.7 | 43.3 | | 60.8 | 68.6 |
| | 88.5 | 50.8 | | 61.9 | 69.6 |
| | 91.1 | 52.9 | | 62.9 | 70.4 |
| | 91.9 | 53.7 | | 63.4 | 70.7 |
| | 92.4* | 54.0* | | 63.7 | 70.9 |
| 0.2476 | 26.1 | 20.3 | | 64.0* | 71.0* |
| | 39.6 | 26.6 | 0.7618 | 27.3 | 50.0 |
| | 53.9 | 36.3 | | 33.4 | 55.9 |
| | 58.9 | 39.6 | | 37.1 | 60.0 |
| | 61.2 | 41.1 | | 41.5 | 65.2 |
| | 72.9 | 49.8 | | 46.1 | 70.2 |
| | 82.8 | 58.3 | | 49.1 | 73.1 |
| | 83.6 | 59.0 | | 49.6* | 73.7* |
| | 84.6 | 59.6 | 0.8964 | 27.8 | 58.3 |
| | 85.0* | 59.8* | | 30.5 | 62.3 |
| 0.4160 | 29.4 | 30.3 | | 32.8 | 65.0 |
| | 39.8 | 36.1 | | 35.0 | 68.2 |
| | 50.6 | 44.5 | | 37.4 | 71.1 |
| | 60.6 | 53.6 | | 38.4 | 72.5 |
| | 70.2 | 62.1 | | 39.2 | 73.5 |
| | 71.0 | 62.9 | | 39.4* | 73.7* |
| | 72.0 | 63.5 | | | |
| | 72.5 | 64.0 | | | |
| | 73.1 | 64.3 | | | |
| | 73.7 | 64.7 | | | |
| | 74.3 | 65.1 | | | |
| | 74.7* | 65.3* | | | |

*Indicate the critical temperature and pressure of the mixture at each $CO_2$ mole fraction.

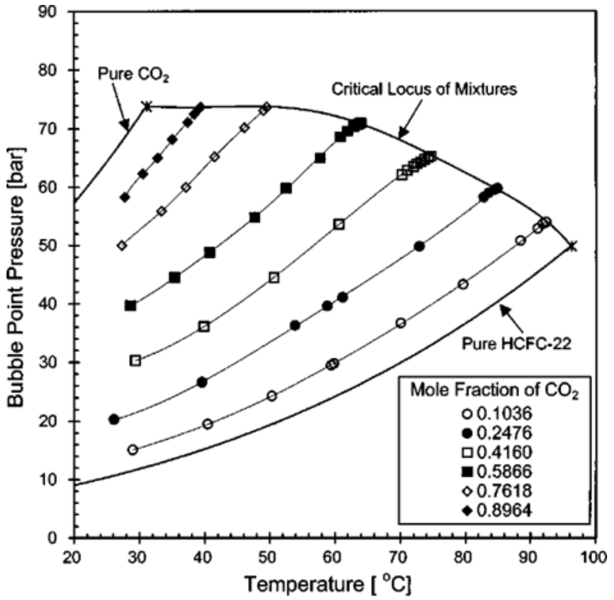


**Fig. 2. Experimental bubble point pressures and critical points of $CO_2$/HCFC-22 mixtures at different mole fractions of $CO_2$.**

bubble point pressure increased as the $CO_2$ content and temperature increased.

The dew point compositions were not measured experimentally in this work, and therefore they should be estimated by a thermodynamic model. We used the well-known Peng-Robinson equation of state (PR-EOS) to calculate the dew point compositions corresponding to the bubble points. The experimental bubble point data were correlated with the PR-EOS which is expressed as follows [Prausnitz et al., 1986]:

$$P=\frac{RT}{v-b}-\frac{a}{v(v+b)+b(v-b)} \quad (1)$$

The mixing rules for the a and b parameters in a mixture are as follows:

$$a_{mix}=\sum_i\sum_j z_i z_j a_{ij} \quad (2)$$

$$a_{ij}=(a_{ii}a_{jj})^{0.5}(1-k_{ij}) \quad (3)$$

**Table 3. Characteristic properties* of $CO_2$ and HCFC-22**

| Compounds | Molecular weight | Critical temperature, $T_c$ [°C] | Critical pressure, $P_c$ [bar] | Acentric factor, ω |
|---|---|---|---|---|
| $CO_2$ | 44.01 | 30.95 | 73.8 | 0.239 |
| HCFC-22 | 86.469 | 96.15 | 49.7 | 0.221 |

*All values are taken from Reid et al. [1987].

$$b_{mix}=\sum_i z_i b_i \quad (4)$$

where $z_i$ is the liquid or vapor phase mole fraction. The above mixing rules contain an adjustable binary interaction parameter, $k_{ij}$, which should be determined by the correlation with the experimental data. The expressions for the $a_{ii}$ and $b_i$ parameters of a pure component are the same as shown in all the textbooks of classical thermodynamics. The expressions for the fugacity coefficients of a component in a mixture required for the VLE calculation of the mixture will not be presented in this paper, since they can be also easily found in the textbooks [Prausnitz et al., 1986; Winnick, 1997]. The characteristic properties of $CO_2$ and HCFC-22 required to calculate the $a_{ii}$ and $b_i$ parameters are given in Table 3 [Reid et al., 1987].

To describe well the VLE by using the PR-EOS, the adjustable binary interaction parameter, $k_{ij}$, given in Eq. (3), should be determined first. In this work the experimental bubble point data were correlated with the PR-EOS [Winnick, 1997]. We used the UNLSF subroutine in the IMSL/Math library to obtain an optimum value of the $k_{ij}$ parameter. When the experimental bubble points (P−x data) at a given temperature were substituted into the PR-EOS, the subroutine found the optimum $k_{ij}$ value by minimizing the following objective function:

$$O.F.=\sum_{i=1}^{m}\left|P_i^{exp}-P_i^{calc}\right| \text{ (m: no. of experimental points)} \quad (5)$$

where $P_i^{exp}$ is the experimental value of pressure and $P_i^{calc}$ is the pressure calculated by the PR-EOS at the experimental bubble point composition.

Using the optimum $k_{ij}$ parameter, the binary VLE (P−xy) was calculated by simultaneously solving the following equilibrium re-

**Table 2. Bubble point pressures at various temperatures estimated by the polynomial interpolation of data given in Table 1**

| Bubble point mole fraction of $CO_2$, $x_1$ | Bubble point pressures [bar] | | | | |
|---|---|---|---|---|---|
| | at 30 °C | at 40 °C | at 50 °C | at 60 °C | at 70 °C |
| 0.0000 | 11.8574* | 15.2593* | 19.3438* | 24.1999* | 29.9259* |
| 0.1036 | 15.4550 | 19.2970 | 24.1168 | 29.9021 | 36.4867 |
| 0.2476 | 21.7235 | 26.9491 | 33.4156 | 40.3934 | 47.6862 |
| 0.4160 | 30.5537 | 36.2026 | 43.9618 | 52.9922 | 61.9980 |
| 0.5866 | 40.5536 | 48.2321 | 57.0579 | 67.6535 | |
| 0.7618 | 52.6739 | 63.4303 | | | |
| 0.8964 | 61.6704 | | | | |
| 1.0000 | 72.1190** | | | | |

*Saturated vapor pressures of pure HCFC-22 obtained from DIPPR of Daubert and Danner (extent 1994).
**Saturated vapor pressure of pure $CO_2$ obtained from DIPPR of Daubert and Danner (extent 1994).

lations:

$$y_i\hat{\phi}_i^v = x_i\hat{\phi}_i^l \quad (i=1,2) \tag{6}$$

where $\hat{\phi}_i^v$ and $\hat{\phi}_i^l$ are the fugacity coefficients of component i in the mixture in vapor and liquid phases, respectively. At an arbitrarily fixed liquid phase mole fraction ($x_1$) and temperature, the system pressure and the vapor phase mole fraction ($y_1$), which satisfied Eq. (6), were calculated. The same calculations were repeated at different liquid phase mole fractions from 0 to 1 with a small interval, and finally a pressure-composition (P–xy) diagram was completed. In these calculations we used the NEQNF subroutine in the IMSL/Math library.

Fig. 3 shows the P–xy diagram calculated by the PR-EOS at several temperatures for the $CO_2$(1)/HCFC-22(2) system along with the experimental points. The bubble point pressure curves (solid lines) and the dew point pressure curves (dashed lines) at temperatures of 40 to 70 °C started from the vapor pressure of pure HCFC-22 and finally met at the critical points of the mixture. The regressed value of the $k_{ij}$ parameter at each temperature is shown in the figure caption. The bubble points calculated by the PR-EOS gave good agreement with those measured experimentally for all temperatures. Figs. 4 to 6 show the critical temperature and pressure of the mixture. The experimentally measured values were taken from Fig. 2 or Table 1, and the calculated values taken from Fig. 3. Good agreement was observed between the experimentally measured critical points and the calculated ones. However, although the results of the bubble and critical points calculated by the PR-EOS showed good agreement with their experimental values, the dew points estimated by the PR-EOS are not guaranteed to be accurate values. Thus, there may exist a difference between the calculated and actual values of the mixture dew points.

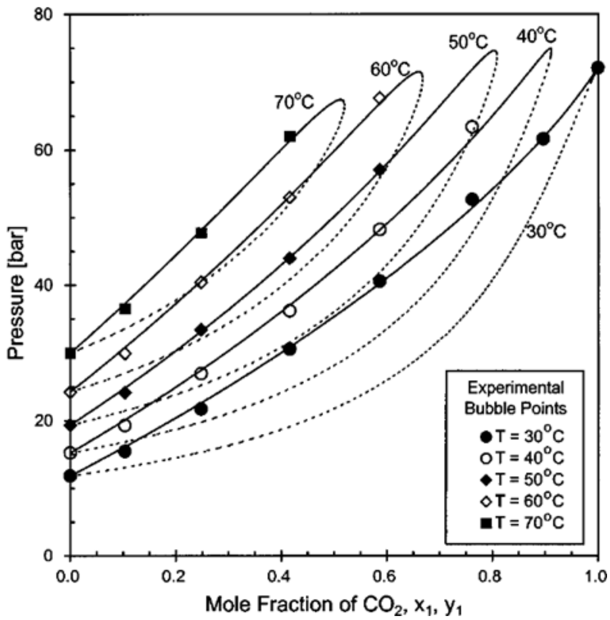


**Fig. 3. P–xy diagram at different temperatures for $CO_2$(1)/HCFC-22(2) system. The symbols are experimental bubble points, and the solid and dashed lines are the bubble point and dew point curves correlated by the PR-EOS, respectively ($k_{ij}$=–0.0024 at 30 °C, –0.0108 at 40 °C, –0.0167 at 50 °C, –0.0047 at 60 °C, –0.0045 at 70 °C).**

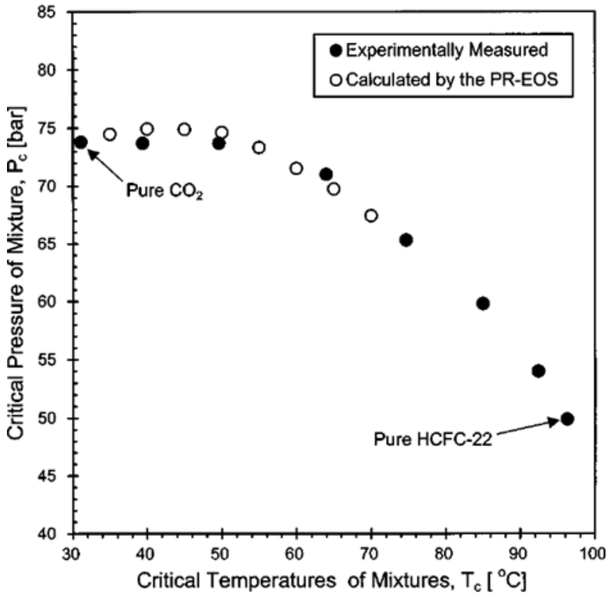


**Fig. 4. Critical pressure and temperature of $CO_2$/HCFC-22 mixtures: a comparison of the experimental and the PR-EOS correlated values.**

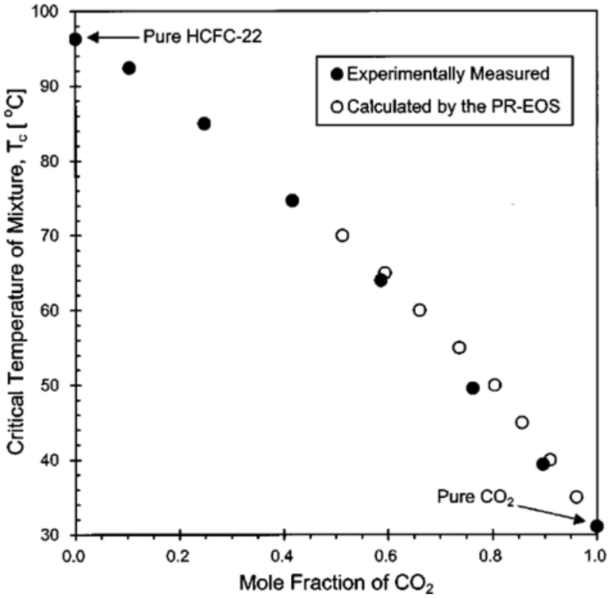


**Fig. 5. Critical temperatures of $CO_2$/HCFC-22 mixtures as a function of $CO_2$ composition: a comparison of the experimental and the PR-EOS correlated values.**

## CONCLUSIONS

The bubble point pressures and the critical points of $CO_2$/HCFC-22 mixtures were measured by using a high-pressure experimental apparatus equipped with a variable-volume view cell, changing the $CO_2$ composition in the range of temperatures above the critical temperature of $CO_2$ and below the critical temperature of HCFC-22. The experimental bubble point pressure data at different tem-

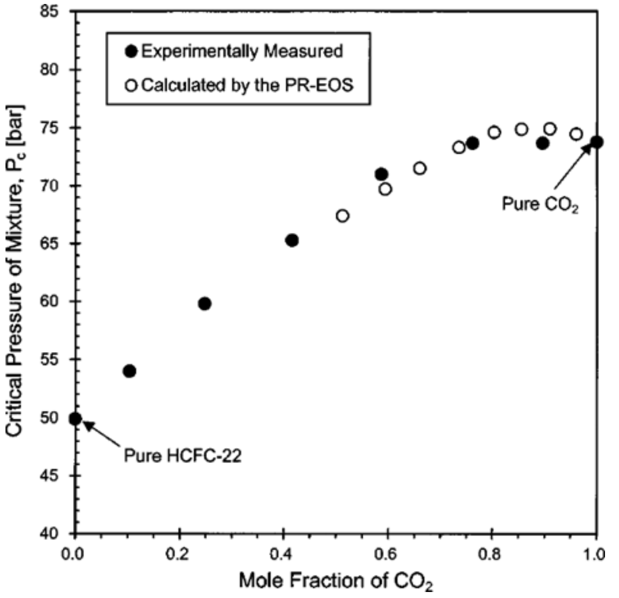


**Fig. 6. Critical pressures of $CO_2$/HCFC-22 mixtures as a function of $CO_2$ composition: a comparison of the experimental and the PR-EOS correlated values.**

peratures were correlated with the Peng-Robinson equation of state to obtain the dew point pressures and compositions in equilibrium with the bubble points. The experimentally measured bubble point pressures and the mixture critical points gave good agreement with those calculated by the PR-EOS. The variable-volume view cell equipment was verified to be an easy and quick way to measure the bubble point pressures and the mixture critical points of high-pressure compressible fluid mixtures.

## ACKNOWLEDGMENT

This work was supported by grant No. (981-1103-011-2) from the Basic Research program of the KOSEF.

## REFERENCES

Choi, E.-J. and Yeo, S.-D., "Critical Properties for Carbon Dioxide+n-Alkane Mixtures Using a Variable-Volume View Cell," *J. Chem. Eng. Data*, **43**, 714 (1998).

Daubert, T. E. and Danner, R. P., "Physical and Thermodynamic Properties of Pure Compounds: Data Compilation," Taylor and Francis, New York (extent 1994).

Haschets, C. W. and Shine, A. D., "Phase Behavior of Polymer-Supercritical Chlorodifluoromethane Solutions," *Macromolecules*, **26**, 5052 (1993).

Irani, C. A. and Cozewith, C., "Lower Critical Solution Temperature Behavior of Ethylene Propylene Copolymers in Multicomponent Solvents," *J. Appl. Polym. Sci.*, **31**, 1879 (1986).

"IMSL Math/Library: Fortran Subroutines for Mathematical Applications," Visual Numerics, Inc., **2**, 868 (1994).

Knapp, H., Döring, R., Oellrich, L., Plöcker, U. and Prausnitz, J. M., "Vapor-Liquid Equilibria for Mixtures of Low Boiling Substances," DECHEMA Chemistry Data Series, Vol. **VI**, DECHEMA (1982).

Lee, S.-H., LoStracco, M. A. and McHugh, M. A., "Cosolvent Effect on the Phase Behavior of Poly(ethylene-co-acrylic acid)-Butane Mixtures," *Macromolecules*, **29**, 1349 (1996).

Lim, J.-S., Lee, B.-C., Kim, J.-D., Lee, Y.-W. and Lee, Y. Y., "Experimental Measurements of Vapor-Liquid Equilibria for Systems Containing CFC and Halon Alternatives," Proceedings of 4th World Conference on Experimental Heat Transfer, Fluid Mechanics and Thermodynamics, June 2-6, Brussels, Belgium, **1**, 525 (1997).

Nishiumi, H., Akita, H. and Akiyama, S., "High Pressure Vapor-Liquid Equilibria for the HFC125-HFC152a System," *Korean J. Chem. Eng.*, **14**, 359 (1997).

Park, S.-B. and Lee, H., "Vapor-Liquid Equilibria for the Binary Monoethanolamine+Water and Monoethanolamine+Ethanol Systems," *Korean J. Chem. Eng.*, **14**, 146 (1997).

Prausnitz, J. M., Lichtenthaler, R. N. and de Azevedo, E. G., "Molecular Thermodynamics of Fluid-Phase Equilibria," 2nd ed., Prentice-Hall Inc., Englewood Cliffs, NJ (1986).

Reid, R. C., Prausnitz, J. M. and Poling, B. E., "The Properties of Gases and Liquids," 4th ed., McGraw-Hill Book Co., New York (1987).

Winnick, J., "Chemical Engineering Thermodynamics," John Wiley & Sons, Inc., New York (1997).